



# Origin of volatile element depletion among carbonaceous chondrites

Jan L. Hellmann<sup>a,\*</sup>, Timo Hopp<sup>a,b</sup>, Christoph Burkhardt<sup>a</sup>, Thorsten Kleine<sup>a</sup>

<sup>a</sup> Institut für Planetologie, University of Münster, Wilhelm-Klemm-Straße 10, 48149 Münster, Germany

<sup>b</sup> Origins Laboratory, Department of the Geophysical Sciences and Enrico Fermi Institute, The University of Chicago, 5734 South Ellis Avenue, Chicago, IL 60637, USA

## ARTICLE INFO

### Article history:

Received 30 March 2020

Received in revised form 2 July 2020

Accepted 29 July 2020

Available online xxxx

Editor: R. Dasgupta

### Keywords:

tellurium

mass-dependent isotope fractionation

chondrule formation

CI-like matrix

two-component model

chondrule-matrix complementarity

## ABSTRACT

Compared to the composition of CI chondrites and the Sun, all other carbonaceous chondrites are variably depleted in volatile elements. However, the origin of these depletions, and how they are related to volatile loss during high-temperature processes within the solar nebula, are unclear. To better understand the processes that caused volatile element fractionations among carbonaceous chondrites, we obtained mass-dependent Te isotopic compositions and Te concentrations for a comprehensive set of samples from the major carbonaceous chondrite groups. The chondrites exhibit well-resolved inter-group Te isotope variations towards lighter isotopic compositions for increasingly volatile-depleted samples. The Te isotopic compositions and concentrations are also correlated with the mass fraction of matrix and with nucleosynthetic  $\epsilon^{54}\text{Cr}$  anomalies. Combined, these correlations indicate mixing between volatile-rich, isotopically heavy, and  $^{54}\text{Cr}$ -rich CI-like matrix with volatile-poor, isotopically light, and  $^{54}\text{Cr}$ -poorer chondrules or chondrule precursors. The Te-Cr isotopic correlation suggests that all carbonaceous chondrites contain CI-like matrix, and that chondrules and this CI-like matrix formed from isotopically distinct material originating from different regions of the disk. The only samples plotting off the Te-Cr correlation are CR chondrites, indicating that CR chondrules formed from different precursor material than chondrules from other carbonaceous chondrites, either because they formed at greater heliocentric distance and/or at a later time. Plots of volatile element abundances versus matrix mass fraction reveal that chondrules/chondrule precursors display CI-chondritic ratios for volatile elements with 50% condensation temperatures below  $\sim 750$  K, with an overall abundance of  $\sim 0.13 \times \text{CI}$ . Mixing between these two components, therefore, naturally results in CI-like ratios for these elements in all carbonaceous chondrites, in spite of different degrees of volatile depletion. A corollary of this observation is that the CI-like ratios of volatile elements in the bulk silicate Earth may result from the accretion of volatile-depleted materials and do not require accretion of CI chondrites themselves.

© 2020 Elsevier B.V. All rights reserved.

## 1. Introduction

Carbonaceous chondrites are among the most primitive materials of the solar system and also are the likely source of Earth's water and highly volatiles (e.g., C, N). As such, carbonaceous chondrites provide important clues about fractionation and mixing processes within the solar protoplanetary disk, the accretion of primitive planetesimals, and also on the volatile accretion history of Earth. Carbonaceous chondrites consist of chondrules, refractory inclusions, metal and sulfides embedded in a fine-grained matrix, where variations in the proportions of these components define the distinct groups of carbonaceous chondrites. Of these, the CI chondrites are chemically most pristine, as their composition

is most similar to that of the solar photosphere (Palme et al., 2014). All other groups of carbonaceous chondrites are depleted in volatile elements [i.e., elements having 50% condensation temperatures ( $T_C$ ) below those of Mg, Si, and Fe (the 'main component') at  $\sim 1300$  K] relative to CI chondrites (Palme et al., 2014).

The origin of these volatile fractionations remains poorly understood. Traditionally, they have been attributed to either incomplete condensation from the solar nebula (e.g., Albarede, 2009; Ciesla, 2008; Wasson and Chou, 1974) or to variable mixing of volatile-rich matrix with volatile-depleted chondrules (i.e., the two-component model) (e.g., Anders, 1964; Larimer and Anders, 1967). Much of the debate between these two models centered around the issue of whether volatile loss from chondrules was important for determining volatile depletions among chondrites, but no consensus has been reached (see summary in Alexander, 2005). More recent studies have shown that the composition of carbonaceous chondrites can be quantitatively reproduced by variable mix-

\* Corresponding author.

E-mail address: jan.hellmann@uni-muenster.de (J.L. Hellmann).

tures of their chemically and isotopically diverse constituents (e.g., Alexander, 2019; Zanda et al., 2018). Such studies have argued that volatile elements in carbonaceous chondrites predominantly derive from CI-like matrix, and that the volatile fractionations among carbonaceous chondrites reflect dilution with other, volatile-free components (Alexander, 2019; Braukmüller et al., 2018). This is consistent with the observation that all carbonaceous chondrites, regardless of the degree of volatile depletion, exhibit CI-like ratios for volatile elements with  $T_C < 750$  K (Braukmüller et al., 2018). However, for some volatile elements (e.g., Zn) carbonaceous chondrites also exhibit a trend towards lighter isotopic compositions in more volatile-depleted samples, suggesting that the volatiles derive from more than one source (e.g., Pringle et al., 2017). Finally, the complementary chemical and isotopic compositions of chondrules and matrix suggest that both components are genetically linked and, as such, do not derive from two distinct sources (e.g., Budde et al., 2016; Hezel and Palme, 2010).

We obtained mass-dependent Te isotopic data and Te concentrations for a comprehensive set of carbonaceous chondrites, with the ultimate goal to better understand the origin of volatile depletions in carbonaceous chondrites. Tellurium isotopes are of considerable interest in this regard, because Te has a lower condensation temperature [ $T_C \approx 700$  K; (Wood et al., 2019)] than many other moderately volatile elements, making it a sensitive tracer of volatile fractionation processes, and because Te concentrations in carbonaceous chondrites gradually decrease in the order CI–CM–(CV, CO)–CK–CR (Braukmüller et al., 2018). Thus, in analogy to Zn, a trend towards lighter Te isotopic compositions from CI to CR chondrites is expected. Fehr et al. (2018) observed a broad trend between Te isotopic fractionation and volatile depletion among carbonaceous chondrites, however, the data from that study also reveal considerable overlap in the Te isotope compositions of distinct carbonaceous chondrite groups. Moreover, Fehr et al. (2018) also observed Te isotope variations among different carbonaceous chondrites of a given group, suggesting that the Te isotope variations cannot solely be attributed to volatile fractionation among the distinct groups. To more systematically investigate the origin of Te isotope variations among carbonaceous chondrites, we obtained mass-dependent Te isotopic data for the six major carbonaceous chondrite groups (CI, CM, CV, CO, CR, CK), the ungrouped chondrite Tagish Lake, and chondrule and matrix-rich separates from the Allende CV3 chondrite. These data provide new insights into the origin of volatile fractionations among carbonaceous chondrites, the role of chondrules and matrix in producing these fractionations, and the nature of carbonaceous chondrite-like bodies accreted by Earth.

## 2. Samples and analytical methods

### 2.1. Samples

Twenty-two bulk carbonaceous chondrites were selected for this study, including two CI chondrites (Ivuna and Orgueil), the ungrouped C2 chondrite Tagish Lake, six CM chondrites (Paris, Cold Bokkeveld, Jbilet Winselwan, Murchison, MET 01070, LON 94101), four CV3 chondrites (Allende, Leoville, Axtell, Vigarano), three CO3 chondrites (DaG 136, NWA 6015, Kainsaz), two CK4 chondrites (NWA 4679 and Maralinga), and four CR2 chondrites (GRA 06100, NWA 1180, NWA 801, Acfer 139). For most samples, aliquots (50–450 mg) were taken from homogeneous bulk powders produced from >2 g pieces. In addition, three chondrule separates and one matrix separate from Allende were analyzed. Chondrules were separated by hand picking under a binocular and were subdivided into two size fractions of 100–1000  $\mu\text{m}$  and >1000  $\mu\text{m}$ . Additionally, a single chondrule of  $\sim 3$  mm diameter was analyzed.

**Table 1**

Tellurium isotopic and concentration data for carbonaceous chondrites and terrestrial samples.

Sample	Classification	Te (ng/g) ( $\pm 2\sigma$ )	N	$\delta^{128/126}\text{Te}$ ( $\pm 2\text{s.d.}$ )
<i>Carbonaceous chondrites</i>				
Orgueil	CI1	2250 $\pm$ 63	5	0.16 $\pm$ 0.01
Ivuna	CI1	2322 $\pm$ 69	6	0.13 $\pm$ 0.02
<b>Mean CI chondrites</b>		<b>2286 <math>\pm</math> 102</b>	<b>2</b>	<b>0.15 <math>\pm</math> 0.04</b>
Tagish Lake	C2-ung.	1669 $\pm$ 42	5	0.11 $\pm$ 0.01
Paris	CM2	1399 $\pm$ 33	5	0.09 $\pm$ 0.02
Murchison	CM2	1493 $\pm$ 47	5	0.07 $\pm$ 0.03
Jbilet Winselwan	CM2	1546 $\pm$ 58	5	0.08 $\pm$ 0.02
Cold Bokkeveld	CM2	1369 $\pm$ 35	5	0.09 $\pm$ 0.02
LON 94101	CM2	1357 $\pm$ 36	5	0.07 $\pm$ 0.02
MET 01070	CM1	1412 $\pm$ 35	6	0.07 $\pm$ 0.03
<b>Mean CM chondrites</b>		<b>1429 <math>\pm</math> 149</b>	<b>6</b>	<b>0.08 <math>\pm</math> 0.02</b>
Allende (MS-B)	CV3	948 $\pm$ 25	4	0.02 $\pm$ 0.02
Allende (MS-A)	CV3	939 $\pm$ 36	5	0.02 $\pm$ 0.01
Leoville	CV3	852 $\pm$ 23	5	0.01 $\pm$ 0.02
Axtell	CV3	947 $\pm$ 25	5	0.00 $\pm$ 0.01
Vigarano	CV3	802 $\pm$ 24	5	−0.01 $\pm$ 0.01
<b>Mean CV chondrites</b>		<b>897 <math>\pm</math> 134</b>	<b>5</b>	<b>0.01 <math>\pm</math> 0.02</b>
NWA 6015	CO3	808 $\pm$ 24	6	−0.02 $\pm$ 0.03
DaG 136	CO3	821 $\pm$ 36	5	−0.03 $\pm$ 0.02
Kainsaz	CO3	840 $\pm$ 24	5	−0.05 $\pm$ 0.02
<b>Mean CO chondrites</b>		<b>823 <math>\pm</math> 32</b>	<b>3</b>	<b>−0.03 <math>\pm</math> 0.03</b>
NWA 4679	CK4	752 $\pm$ 33	5	0.82 $\pm$ 0.01
Maralinga	CK4	761 $\pm$ 20	5	−0.19 $\pm$ 0.03
GRA 06100	CR2	762 $\pm$ 22	5	−1.38 $\pm$ 0.02
NWA 1180	CR2	481 $\pm$ 12	6	−0.20 $\pm$ 0.03
Acfer 139	CR2	489 $\pm$ 12	4	−0.21 $\pm$ 0.03
NWA 801	CR2	511 $\pm$ 12	6	−0.24 $\pm$ 0.02
<b>Mean CR chondrites</b>		<b>494 <math>\pm</math> 31</b>	<b>3</b>	<b>−0.22 <math>\pm</math> 0.04</b>
<i>Allende components</i>				
Pooled chondrules 100–1000 $\mu\text{m}$		327 $\pm$ 14	3	−0.03 $\pm$ 0.01
Pooled chondrules >1000 $\mu\text{m}$		305 $\pm$ 11	3	−0.04 $\pm$ 0.02
Single chondrule 3 mm		558 $\pm$ 37	1	0.03 $\pm$ 0.03
Matrix-rich		1102 $\pm$ 36	3	0.01 $\pm$ 0.01
<i>Terrestrial standards</i>				
BHVO-2	Basalt	14.5 $\pm$ 0.6	3	0.25 $\pm$ 0.03
UB-N	Serpentine	11.0 $\pm$ 0.7	3	0.05 $\pm$ 0.01
SBC-1	Shale	146 $\pm$ 3	5	−0.06 $\pm$ 0.03
Nod-A-1	Mn-nodule	29589 $\pm$ 766	5	0.44 $\pm$ 0.02
Nod-P-1	Mn-nodule	4949 $\pm$ 154	5	0.31 $\pm$ 0.02

Some samples were provided by NASA (LON 94101.72, MET 01070.47, GRA 06100.58), IPGP (Paris), and the Field Museum (Murchison ME 2644.25.1).

For comparison to previous studies we also obtained Te isotopic data for some readily available reference samples: basalt BHVO-2, serpentine UN-B, shale SBC-1, and Mn-nodules Nod-A-1 and Nod-P-1 (Table 1). Although no prior studies reported Te isotopic data for the first three of these samples, they may serve as appropriate reference materials for inter-study comparison in the future. Two previous studies reported Te stable isotopic data for the Mn-nodules Nod-A-1 and Nod-P-1, obtained by double spike MC-ICPMS (Fehr et al., 2018; Fukami et al., 2018). Comparison of data from this and previous studies, including terrestrial samples and chondrites, generally reveals a good agreement between the studies, although there seems to be a small systematic offset compared to the results of Fehr et al. (2018), which most likely reflects the use of different standards (see supplement for details).

### 2.2. Tellurium double spike

Tellurium has eight stable isotopes, and so there are several possibilities for the design of the double spike. Contrary to previous studies, which used a  $^{125}\text{Te}$ – $^{128}\text{Te}$  double spike (Fehr et al., 2018; Fukami et al., 2018), we chose a  $^{123}\text{Te}$ – $^{125}\text{Te}$  double spike

with an isotopic composition optimized for using  $^{123}\text{Te}$ ,  $^{125}\text{Te}$ ,  $^{126}\text{Te}$ , and  $^{128}\text{Te}$  in the inversion. The  $^{123}\text{Te}$ – $^{125}\text{Te}$  double spike was prepared from  $^{123}\text{Te}$  (~2 mg; batch no. 208940) and  $^{125}\text{Te}$  (~5 mg; batch no. 192046) single spikes purchased from the Oak Ridge National Laboratory. The final double spike was calibrated against the NIST SRM 3156 Te standard solution (Lot No. 140830;  $10.005 \pm 0.038 \text{ mg g}^{-1} \text{ Te}$ ), which is used as the reference standard throughout this study.

The  $^{123}\text{Te}$ – $^{125}\text{Te}$  double spike setup has a small predicted error (1s.d.) of ~33 ppm amu $^{-1}$  (Rudge et al., 2009) and a relatively broad range of permissible spike-to-sample ratios (Fig. S1). The use of a  $^{123}\text{Te}$ – $^{125}\text{Te}$  double spike has the advantage that it avoids  $^{130}\text{Te}$ , which has been shown to be prone to analytical artifacts (Brennecka et al., 2017). Although  $^{126}\text{Te}$  and  $^{128}\text{Te}$  may be affected by interferences from Xe, the Xe background is very constant and can reliably be corrected by on-peak background measurements prior to each analysis. Finally, Sb, which interferes with  $^{123}\text{Te}$ , is efficiently removed during chemical purification and the amount of any remaining  $^{123}\text{Sb}$  is sufficiently low ( $^{121}\text{Sb}/^{123}\text{Te} < 1.4 \times 10^{-3}$ ) for reliable correction using the interference-free  $^{121}\text{Sb}$  (Fig. S2).

### 2.3. Sample preparation and chemical separation of Te

Samples were weighed into 15 or 60 ml Savillex PFA vials and mixed with appropriate amounts of  $^{123}\text{Te}$ – $^{125}\text{Te}$  double spike. The sample-spike mixtures were dissolved in 2:1 HF–HNO $_3$  on a hot plate for 2–3 days at 120–150 °C. After dissolution, samples were evaporated to dryness at 120 °C and the residues were taken up and dried several times in concentrated HNO $_3$  to destroy fluorides that may have formed during digestion. The samples were then converted to chloride form by several dry downs in concentrated HCl, and re-dissolved in 25 mL 2 M HCl for ion exchange chemistry.

Tellurium was purified using a three-stage column chemistry modified following the procedures of Fehr et al. (2004) and Brennecka et al. (2017). First, sample solutions in 2 M HCl were loaded onto pre-cleaned anion exchange columns filled with 5 mL Bio-Rad AG1X8 resin (200–400 mesh). After loading, the columns were washed sequentially with 15 mL 2 M HCl, 7 mL 11 M HCl, and 15 mL 5 M HF, and Te was eluted in 10 mL 1 M HNO $_3$ . The Te fractions were dried on a hot plate with added concentrated HNO $_3$  to destroy organic compounds. This was followed by several dry downs in concentrated HCl to remove remaining HNO $_3$ . The Te fractions were then dissolved in 1 mL 2 M HCl and loaded onto a clean-up column filled with 1 mL pre-cleaned BioRad AG1X8 resin (200–400 mesh). After loading, the columns were washed sequentially with 5 mL 2 M HCl, 2 mL 11 M HCl, and 5 mL 5 M HF. Afterwards, Te was eluted using 6 mL 0.5 M HCl. The Te fractions from the second chemistry were dried several times in HNO $_3$  and then dissolved in 1 mL 7 M HNO $_3$ . Finally, to remove any remaining Mo from the Te fractions, sample solutions were loaded onto pre-cleaned columns (500  $\mu\text{l}$  TRU resin-B, 50–100  $\mu\text{m}$ ) and Te was directly collected together with an additional elution of further 4 mL 7 M HNO $_3$ . After dry downs in HNO $_3$  and HNO $_3$ –HCl, the Te fractions were dissolved in 0.28 M HNO $_3$  for isotope measurements.

### 2.4. Mass spectrometry and data reduction

All Te isotope measurements were performed using a ThermoScientific Neptune Plus multi-collector ICP-MS at the Institut für Planetologie. Samples were introduced using a Cetac Aridus II desolvator and a Savillex C-flow nebulizer at an uptake rate of ~40  $\mu\text{l}/\text{min}$ . Sample solutions were measured at ~100 ppb Te (except the chondrule separates, BHVO-2, and UB-N, which were measured at ~30–50 ppb Te) using standard sampler and X skimmer

cones. For a 100 ppb standard solution this configuration yielded total ion beam intensities of ~2–2.5  $\times 10^{-10}$  A. Ion beams were collected simultaneously using Faraday cups connected to  $10^{11}$   $\Omega$  feedback resistors for  $^{123}\text{Te}$ ,  $^{125}\text{Te}$ ,  $^{126}\text{Te}$ , and  $^{128}\text{Te}$ , and Faraday cups connected to  $10^{12}$   $\Omega$  feedback resistors for  $^{121}\text{Sb}$  and  $^{129}\text{Xe}$ . Prior to each analysis the sample introduction system was washed using 0.28 M HNO $_3$  for 10–15 min. Each measurement consisted of on-peak zero measurements of  $100 \times 1.05$  s integrations, followed by sample measurements of 50 cycles of 4.2 s each. Interferences of Xe on  $^{126}\text{Te}$  and  $^{128}\text{Te}$ , and of Sb on  $^{123}\text{Te}$  were corrected by monitoring  $^{129}\text{Xe}$  and  $^{121}\text{Sb}$  and using the exponential mass fractionation law, but corrections were insignificant for most samples.

The measured raw data were processed off-line following the three-dimensional data reduction routine of Siebert et al. (2001), and using  $^{123}\text{Te}/^{128}\text{Te}$ ,  $^{125}\text{Te}/^{128}\text{Te}$ , and  $^{126}\text{Te}/^{128}\text{Te}$ . The double spike inversion provides the natural fractionation factor  $\alpha$ , from which the Te isotope fractionation (in permil) of a sample is calculated as follows:

$$\delta^{128/126}\text{Te}_{\text{sample}} = -1000 \times (\alpha_{\text{sample}} - \alpha_{\text{Mean NIST SRM3156}}) \times \ln(m_{128}/m_{126}) \quad (1)$$

where  $m_{128}$  and  $m_{126}$  are the atomic weights of  $^{128}\text{Te}$  and  $^{126}\text{Te}$ , and  $\alpha_{\text{Mean NIST SRM 3156}}$  is the mean natural fractionation factor  $\alpha$  of an optimally spiked NIST SRM 3156 standard solution (spike proportion of 0.40) measured at similar concentrations in the same measurement sequence. The long-term reproducibility of spiked standard solutions at ~100 ppb obtained during the course of this study is  $\pm 0.023\text{‰}$  (2s.d.) (Fig. S3). The results for samples are reported as the mean of pooled solution replicates ( $n = 3\text{--}8$ ) with their corresponding two standard deviation (2s.d.).

The double spike inversion assumes that the samples have no mass-independent Te isotope anomalies, and so if such anomalies would exist, then inaccurate mass fractionation factors may be calculated (e.g., Hopp and Kleine, 2018). Although no mass-independent Te isotope anomalies have yet been found (Fehr et al., 2006), it is nevertheless important to assess how large such anomalies would have to be to significantly affect the calculated  $\delta^{128/126}\text{Te}$ . To this end, we calculated the apparent  $\delta^{128/126}\text{Te}$  of an artificial sample for which we assumed an  $s$ -process deficit corresponding to a  $\epsilon^{126}\text{Te}$  anomaly of  $-0.3$  (the  $\epsilon$  notation expresses the parts per 10,000 deviation of a mass fractionation corrected isotopic ratio in a sample relative to a standard). Such an anomaly is similar to the uncertainty of  $\pm 0.3$  on  $\epsilon^{126}\text{Te}$  (Fehr et al., 2006), and therefore is the largest nucleosynthetic Te isotope anomaly that may exist based on currently available data. The calculation shows that this would change the calculated  $\delta^{128/126}\text{Te}$  by ~0.03‰, which is similar to the precision of the Te isotope measurements of this study and much smaller than the observed  $\delta^{128/126}\text{Te}$  variations among the carbonaceous chondrites. Consequently, mass-independent Te isotope anomalies, if they exist, have no significant effect on the  $\delta^{128/126}\text{Te}$  data reported here.

## 3. Results

Tellurium concentrations and  $\delta^{128/126}\text{Te}$  values of bulk carbonaceous chondrites and Allende chondrule and matrix fractions are provided in Table 1 (and Table S1 using the  $\delta^{130/125}\text{Te}$ -notation to facilitate direct comparison to a prior study) and are shown on Figs. 1 and 2. With the exception of the CR2 chondrite GRA 06100 ( $\delta^{128/126}\text{Te} \approx -1.38\text{‰}$ ) and the CK4 chondrite NWA 4679 ( $\delta^{128/126}\text{Te} \approx +0.82\text{‰}$ ), all samples display a narrow range of ~0.4‰ for  $\delta^{128/126}\text{Te}$ . For CI, CM, CV, CO, and CR chondrites (except GRA 06100), samples from a given carbonaceous chondrite group have indistinguishable  $\delta^{128/126}\text{Te}$  and display a narrow range

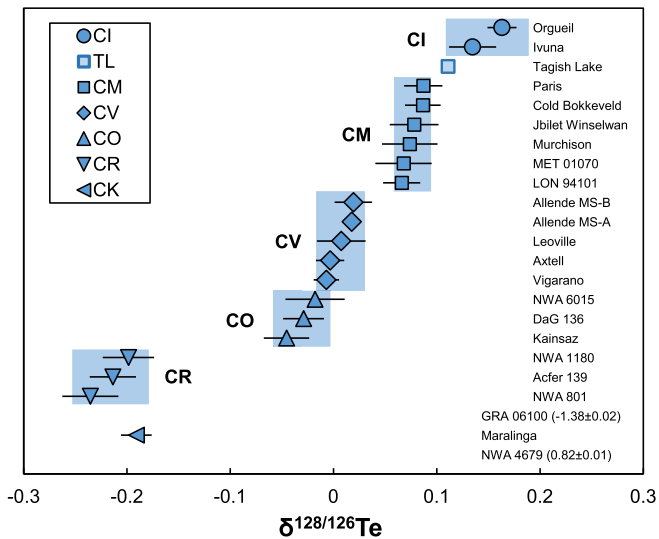


**Fig. 1.**  $\delta^{128/126}\text{Te}$  data of carbonaceous chondrites. Blue bars represent the 2s.d. of each carbonaceous chondrite group. Samples NWA 4679 (CK4) and GRA 06100 (CR2) plot off scale. (For interpretation of the colors in the figure(s), the reader is referred to the web version of this article.)

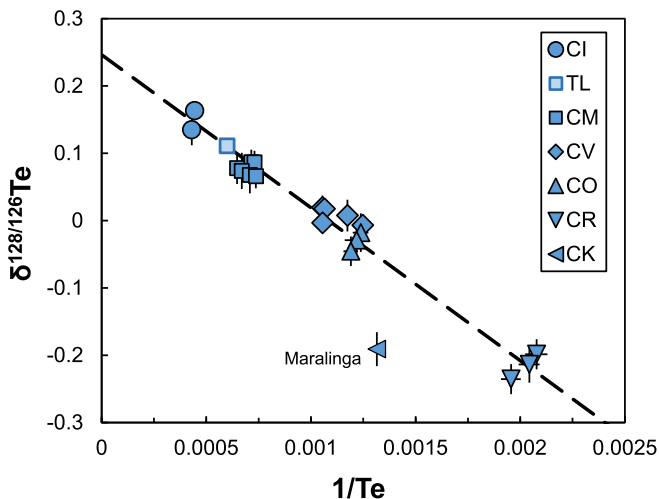


**Fig. 2.**  $\delta^{128/126}\text{Te}$  and  $1/\text{Te}$  data for carbonaceous chondrites. TL: Tagish Lake. GRA 06100 (CR2), NWA 4679 (CK4) plot off scale. These two chondrites and Maralinga (CK4) are the only samples of this study that do not plot on the  $\delta^{128/126}\text{Te}$ - $1/\text{Te}$  correlation line.  $1/\text{Te}$  was calculated using Te concentrations in  $\text{ng g}^{-1}$ .

of Te concentrations. Among these groups, and including the ungrouped carbonaceous chondrite Tagish Lake,  $\delta^{128/126}\text{Te}$  and Te concentrations vary systematically, where CI chondrites display the heaviest  $\delta^{128/126}\text{Te}$  and highest Te concentrations, while CR chondrites have the lightest  $\delta^{128/126}\text{Te}$  and lowest Te concentrations (Figs. 1, 2). This is consistent with results from a previous study, which showed a broad trend towards increasingly heavy Te isotopic signatures for more volatile-rich carbonaceous chondrites (Fehr et al., 2018). The new data of this study, however, are based on a larger and more diverse sample set and allow to define the correlation of isotopic composition with volatile content much more precisely (see Fig. S4 for details).

Of the bulk carbonaceous chondrites analyzed in this study, only the two CK4 chondrites and the CR2 chondrite GRA 06100 deviate from the trend of  $\delta^{128/126}\text{Te}$  with Te concentration defined by the other carbonaceous chondrites (Fig. 2). Prior studies have shown that thermal and shock metamorphism may induce isotope fractionations for Te (Fehr et al., 2018), resulting in both light and heavy isotopic compositions. Although CR chondrites are typically

not strongly affected by thermal metamorphism on their parent body, GRA 06100 provides evidence for substantial thermal processing, most likely as a consequence of shock-heating to  $>600^\circ\text{C}$  during an impact event (Abreu and Bullock, 2013; Briani et al., 2013). This event may have resulted in Te isotope fractionation and, therefore, may account for the anomalous Te systematics of GRA 06100, as has also been observed for Zn and Cd isotopes in this sample (Mahan et al., 2018; Toth et al., 2020). The deviation of the two CK chondrites from the overall  $\delta^{128/126}\text{Te}$  versus Te trend most likely also reflects the effects of thermal processing on the parent body. Unlike many other carbonaceous chondrites, most CK chondrites show evidence of thermal metamorphism (Geiger and Bischoff, 1991), which may have induced large Te isotope variations due to thermal diffusion. As such, the measured  $\delta^{128/126}\text{Te}$  of the CK4 chondrites most likely do not represent that of their parent body. Therefore, the data for the CR chondrite GRA 06100 and the two CK chondrites will not be further considered when using the Te isotopic data to understand volatile fractionations among carbonaceous chondrite groups.

Unlike a previous study (Fehr et al., 2018), we do not observe variable  $\delta^{128/126}\text{Te}$  among samples of a given carbonaceous chondrite group (except for the aforementioned CKs and the CR chondrite GRA 06100) (Fig. 1). This not only makes it possible to precisely define the  $\delta^{128/126}\text{Te}$  for each group, but also implies that for these chondrite groups parent body processes had no significant effect on the Te stable isotopic composition of bulk samples, at least not for the sample sizes used in this study. For instance, the six CM chondrites of the present study were subject to different degrees of aqueous alteration (petrologic types 1–2.9), but nevertheless display indistinguishable  $\delta^{128/126}\text{Te}$ . Further, the four different CV3 chondrites have been subject to different degree of thermal processing on the parent body (Bonal et al., 2006), yet have indistinguishable  $\delta^{128/126}\text{Te}$ . Thus, thermal processing on the CV3 parent body does not seem to have modified  $\delta^{128/126}\text{Te}$ , at least not at the bulk rock scale. The two CI, three CO, and three CR chondrites (excluding GRA 06100) of this study also have consistent  $\delta^{128/126}\text{Te}$  values, which we interpret to represent those of their respective parent bodies.

Finally, the two pooled Allende chondrule separates and the single Allende chondrule have lower Te concentrations than bulk Allende. The single chondrule displays a similar  $\delta^{128/126}\text{Te}$  value than bulk Allende, whereas the two pooled chondrule separates have slightly lighter isotopic compositions. Finally, the matrix-rich sample has a higher Te concentration than bulk Allende, but the same  $\delta^{128/126}\text{Te}$  (Table 1).

## 4. Discussion

### 4.1. Correlation of $\delta^{128/126}\text{Te}$ with matrix fraction

The CI, CM, CV, CO, and CR chondrites together with Tagish Lake define a single precise linear trend in a plot of  $\delta^{128/126}\text{Te}$  versus  $1/\text{Te}$  (Fig. 2), indicating that the depletion of Te is associated with isotopic fractionation towards lighter isotopic compositions. This is consistent with prior observations for some other volatile elements (in particular Zn), which also show lighter isotopic compositions for more volatile depleted samples (Pringle et al., 2017). The  $\delta^{128/126}\text{Te}$  values and Te concentrations are not only correlated with one another, but also with the volume fraction of matrix of each chondrite group (Fig. 3). Assessing this observation more quantitatively requires converting matrix volume fractions ( $\phi$ ) into mass fractions ( $\omega$ ). To this end, we assumed that all material except chondrules (Ch), refractory inclusions (RI), metal (M), and sulfides (S) belongs to matrix. The matrix mass fraction is then given by:

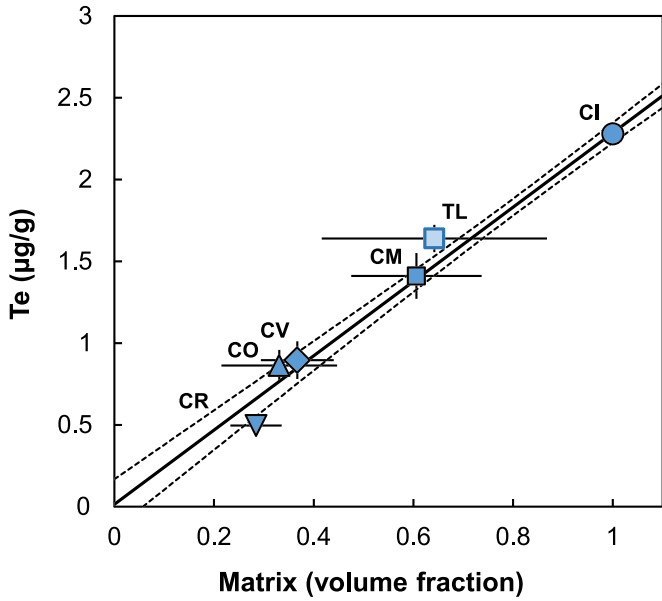


**Fig. 3.** Average Te concentration of carbonaceous chondrite groups versus volume fraction of matrix. Matrix volume fractions taken from summary in Alexander (2019). Uncertainties are two times the standard deviation and dashed lines represent the corresponding error envelope of the linear regression.

$$\omega_{matrix} = 1 - (\omega_{Ch} + \omega_{RI} + \omega_M + \omega_S) \quad (2)$$

The mass fraction  $\omega_i$  of each component can be obtained from their volume fractions:

$$\omega_i = \phi_i \times \frac{\rho_i}{\rho_{bulk}} \quad (3)$$

where  $\rho_{bulk}$  is the bulk density of a given chondrite (Macke et al., 2011) and  $\rho_i$  is the density of a given component. We assumed  $\rho = 3.3 \text{ g cm}^{-3}$  for chondrules and refractory inclusions,  $8.0 \text{ g cm}^{-3}$  for FeNi-metal, and  $4.6 \text{ g cm}^{-3}$  for sulfides (EngToo, 2001). For CV and CO chondrites we used volume fractions from McSween (1977a, 1977b), resulting in matrix mass fractions of  $0.30 \pm 0.07$  and  $0.20 \pm 0.12$  (2s.d.), respectively. For CR chondrites, volume fractions were taken from Schrader et al. (2011), resulting in a matrix mass fraction of  $0.09 \pm 0.05$  (2s.d.). Note that the high metal contents of ~5–8 vol.% of CR chondrites results in a drastically lower matrix mass fractions compared to the volume fraction (~25–35 vol.%). For CM chondrites, volume fractions are highly variably (e.g., 57–85 vol.% matrix), most likely as a result of aqueous alteration on the parent body (Marrocchi et al., 2014; McSween, 1979). We, therefore, used volume fractions from the least altered CM chondrites, such as Crescent, Mighei, Murray, Murchison, and Paris (which contain ~60 vol.% matrix). For these samples, a matrix mass fraction of  $0.41 \pm 0.12$  (2s.d.) is calculated. Finally, the ungrouped chondrite Tagish Lake has also been subject to extensive aqueous alteration, and so conversion of volume to mass fraction is more difficult for this sample. Moreover, observed volume matrix fractions are highly variable among different subsamples of Tagish Lake [0.50–0.90; Blinova et al. (2014)]. Nevertheless, the low grain density of  $2.74 \text{ g cm}^{-3}$  of Tagish Lake (Hildebrand et al., 2006) suggests that aqueous alteration lowered the densities of all other components to about the same value. In this case, the matrix volume fraction is equivalent to its mass fraction, resulting in a mass fraction of  $0.64 \pm 0.23$  (2s.d.).

The matrix mass fractions thus obtained are linearly correlated with the Te concentrations of the carbonaceous chondrites, indicating that the variable Te concentrations reflect different amounts of Te-rich matrix (Fig. 4). The Te concentration of the Te-poor, non-matrix component, as inferred from the intercept at a matrix

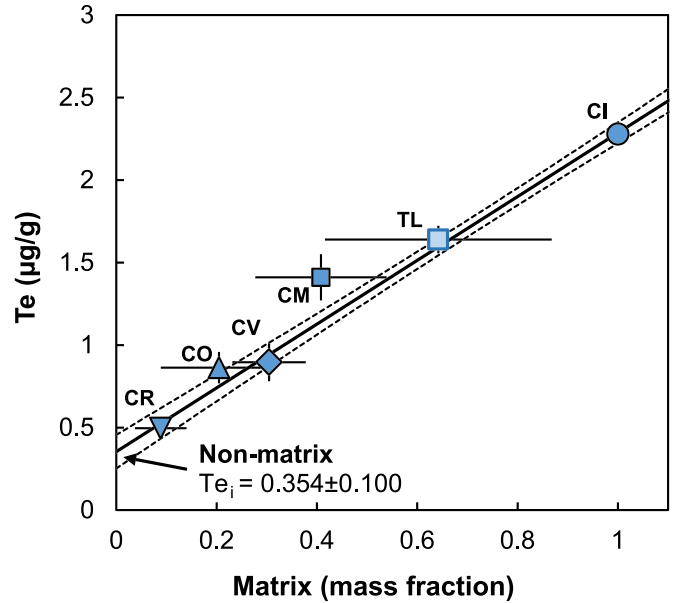


**Fig. 4.** Average Te concentration of carbonaceous chondrite groups versus mass fraction of matrix (see section 4.1 for details). The regression represents the best fit using weighted errors. The y-axis intercept of the regression provides the Te concentration of the non-matrix component. Uncertainties are two standard deviations and dashed lines represent the corresponding error envelope of the linear regression.

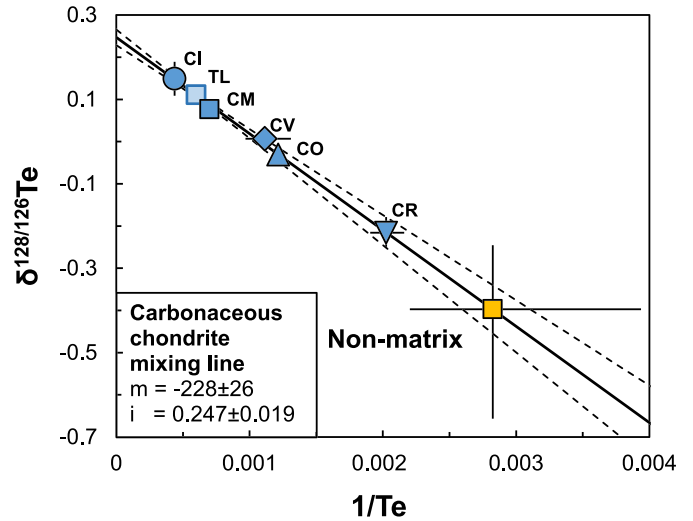


**Fig. 5.**  $\delta^{128/126}\text{Te}-1/\text{Te}$  mixing line defined by carbonaceous chondrite groups. TL: Tagish Lake. The Te isotopic composition of the non-matrix component was determined using the inferred Te concentration (see section 4.1) and the  $\delta^{128/126}\text{Te}-1/\text{Te}$  regression of carbonaceous chondrite groups. The regression represents the best fit using weighted errors. Uncertainties are two standard deviation and dashed lines represent the corresponding error envelope of the linear regression.  $1/\text{Te}$  was calculated using Te concentrations in  $\text{ng g}^{-1}$ .

mass fraction of zero, is  $354 \pm 100 \text{ ng g}^{-1}$ . Using this Te concentration, the  $\delta^{128/126}\text{Te}$  value of the non-matrix component can be estimated from the  $\delta^{128/126}\text{Te}-1/\text{Te}$  correlation, yielding  $\delta^{128/126}\text{Te} = -0.40^{+0.15}_{-0.26}$  for the non-matrix component (Fig. 5). This component must be represented by either metal, chondrules, or refractory inclusions. Metal does not occur in sufficiently variable amounts in the carbonaceous chondrite groups, and so the non-matrix component is probably represented by chondrules and/or refractory inclusions. Of note, several prior studies have shown that chondrules and also CAIs have isotopically light compositions for volatile elements such Zn, Ga, and Cd (Kato and Moynier, 2017; Pringle et al., 2017; Van Kooten and Moynier, 2019; Wombacher

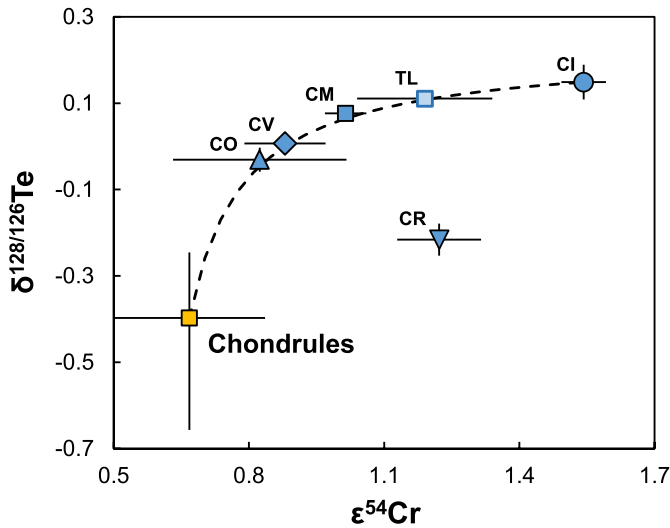


**Fig. 6.**  $\delta^{128/126}\text{Te}$  versus  $\epsilon^{54}\text{Cr}$  for carbonaceous chondrites. For sources of  $^{54}\text{Cr}$  data see Table S3.

et al., 2008). The Te isotopic data from this study also reveal light  $\delta^{128/126}\text{Te}$  for two pooled chondrule separates from the CV3 chondrite Allende, but these are not as light as the composition of the non-matrix component inferred above. However, the  $\delta^{128/126}\text{Te}$  of Allende chondrules may have been modified by parent body processes, and so the Te isotopic composition of physically separated non-matrix components may provide less stringent constraints on their original isotopic composition than the precisely defined correlation of  $\delta^{128/126}\text{Te}$  and  $1/\text{Te}$  among the bulk carbonaceous chondrites. In other words, the evidence for light isotopic compositions of non-matrix material may be preserved only indirectly, by the volatile element depletion trend of bulk carbonaceous chondrites towards light isotopic compositions.

#### 4.2. $\delta^{128/126}\text{Te}-\epsilon^{54}\text{Cr}$ correlation

The  $\delta^{128/126}\text{Te}$  values of carbonaceous chondrites (except CR) are not only correlated with Te concentrations and matrix mass fraction, but also with  $\epsilon^{54}\text{Cr}$  (Fig. 6). This correlation is remarkable because variations in  $\delta^{128/126}\text{Te}$  and  $\epsilon^{54}\text{Cr}$  have different origins. While the former reflect thermal and chemical processing of chondrite precursors, variations in  $\epsilon^{54}\text{Cr}$  are nucleosynthetic in origin and reveal that different groups of carbonaceous chondrites incorporated variable amounts of presolar materials (Trinquier et al., 2007). The  $\delta^{128/126}\text{Te}-\epsilon^{54}\text{Cr}$  correlation, therefore, indicates that the different carbonaceous chondrites cannot have formed by processing from the same homogeneous reservoir of dust. The correlated  $\delta^{128/126}\text{Te}-\epsilon^{54}\text{Cr}$  variations may reflect that dust in more distant regions of the disk, which was characterized by more elevated  $\epsilon^{54}\text{Cr}$  (e.g., the formation location of CI and CM chondrites) underwent less severe thermal processing than dust in more proximal regions, which was characterized by less positive  $\epsilon^{54}\text{Cr}$  (e.g., the formation location of CV and CO chondrites). This would be consistent with the different amounts of matrix in these chondrites, because larger amounts of matrix may be indicative of less efficient chondrule formation. In this case, the  $\delta^{128/126}\text{Te}-\epsilon^{54}\text{Cr}$  correlation would reflect coherent gradients of thermal processing (as reflected in  $\delta^{128/126}\text{Te}$ ) and compositional changes (as reflected in  $\epsilon^{54}\text{Cr}$ ) in the disk, without a direct causal relationship between  $\delta^{128/126}\text{Te}$  and  $\epsilon^{54}\text{Cr}$ .

Alternatively, the correlated  $\delta^{128/126}\text{Te}-\epsilon^{54}\text{Cr}$  variations among carbonaceous chondrites reflect mixing of two isotopically distinct components. One of these components is CI-like matrix, which is volatile-rich, isotopically heavy for Te, and enriched in  $^{54}\text{Cr}$ . The

other, non-matrix component is volatile-depleted, isotopically light for Te, and has smaller  $\epsilon^{54}\text{Cr}$  anomalies. Of note, most refractory inclusions (CAIs, AOAs) are characterized by  $\epsilon^{54}\text{Cr}$  values of  $\sim 6$  (Trinquier et al., 2009), and so cannot represent the non-matrix endmember (Fig. 6). Instead, chondrules from CV, CO, and CM chondrites, in spite of large variations among individual chondrules in each group, are characterized by an average  $\epsilon^{54}\text{Cr}$  of  $\sim 0.7$  (Fig. S5, Table S3). Chondrules with this average  $\epsilon^{54}\text{Cr}$  and a  $\delta^{128/126}\text{Te}$  of about  $-0.40$  (as inferred above) plot on the  $\delta^{128/126}\text{Te}-\epsilon^{54}\text{Cr}$  mixing line of bulk carbonaceous chondrites, and mixing calculations between chondrules and CI chondrites reproduce the observed compositions of bulk carbonaceous chondrites quite well (Fig. 6). Together, these observations are consistent with the interpretation of the  $\delta^{128/126}\text{Te}-\epsilon^{54}\text{Cr}$  covariation as a mixing line between chondrules (or chondrule precursors) and CI-like matrix. A corollary of this is that all carbonaceous chondrites (except possibly the CRs) contain CI-like matrix, which in turn is consistent with CI-like matrix-normalized abundances of organic matter and presolar grains in the most primitive samples from each chondrite group (Alexander, 2005; Alexander et al., 2001).

The  $\delta^{128/126}\text{Te}-\epsilon^{54}\text{Cr}$  covariation defined by CO-CV-CM-CI chondrites and Tagish Lake implies that chondrules in these chondrites formed from the same or similar precursor material. Otherwise, these chondrites would not plot on a single mixing line with an average  $\epsilon^{54}\text{Cr}$   $\sim 0.7$  for chondrules as one endmember. This is consistent with the aforementioned observation that chondrules from CV, CO, and CM chondrites have the same average  $\epsilon^{54}\text{Cr}$  of  $\sim 0.7$ . As this value is distinct from CI chondrites ( $\epsilon^{54}\text{Cr} \sim 1.6$ ), chondrules cannot have formed from CI-like dust, because chondrule melting is not expected to result in nucleosynthetic isotope variations (Jacquet et al., 2019). Instead, the distinct  $\epsilon^{54}\text{Cr}$  of chondrules and CI chondrites imply that chondrule precursors and CI-like matrix derive from different areas of the disk, and were mixed together in various proportions prior to chondrite accretion. This mixing may have occurred naturally within the disk through the inward drift of gas and (CI-like) dust towards the Sun, and it may have taken place before, during, or after chondrule formation. Note that although at least some portion of the matrix has never been involved in any heating event (Alexander, 2005), this does not necessarily mean that the CI-like matrix was mixed with chondrules after their formation. It is also possible that this mixing occurred earlier (i.e., between chondrule precursors and CI-like dust) and that chondrule formation occurred more locally, so that much of the surrounding dust remained unaffected by the chondrule heating event(s) (Desch et al., 2005).

The CR chondrites are the only chondrites of this study that plot off the  $\delta^{128/126}\text{Te}-\epsilon^{54}\text{Cr}$  mixing line (Fig. 6). CR chondrules also display a much higher  $\epsilon^{54}\text{Cr}$  of  $\sim 1.4$  compared to CV, CM, and CO chondrules (Olsen et al., 2016), indicating that CR chondrules formed from different precursor material than the other chondrules. Nevertheless, as CR chondrites plot on the same  $\delta^{128/126}\text{Te}-1/\text{Te}$  mixing line together with all other carbonaceous chondrites, the volatile depletion of CR chondrites was likely caused by the same processes and occurred under similar conditions than in other carbonaceous chondrites. Consequently, CR chondrites plot off the  $\delta^{128/126}\text{Te}-\epsilon^{54}\text{Cr}$  mixing line because their chondrules formed from different precursor material than the other chondrules. This is consistent with the idea that CR chondrites formed at greater heliocentric distance (Van Kooten et al., 2020) and/or at a later time (Budde et al., 2018) than most other carbonaceous chondrites.

#### 4.3. Chondrule-matrix complementarity

At first sight the presence of CI-like matrix in all carbonaceous chondrites, and derivation of chondrule precursors and ma-

trix from different areas of the disk, appears inconsistent with the complementary isotopic and chemical compositions of chondrules and matrix (Budde et al., 2016; Hezel and Palme, 2010). In brief, complementarity is defined as complementary chemical or isotopic enrichments and depletions in chondrules and matrix relative to a well-defined (and approximately constant) bulk composition. For instance, bulk carbonaceous chondrites have approximately constant Mg/Si ratios, whereas chondrules typically have superchondritic Mg/Si and matrix has subchondritic Mg/Si. This indicates that no appreciable amounts of chondrules or matrix were lost, because otherwise the Mg/Si of bulk carbonaceous chondrites would have changed. Similarly, chondrules from the CV3 chondrite Allende are characterized by  $\epsilon^{183}\text{W}$  excesses, whereas matrix has  $\epsilon^{183}\text{W}$  deficits (Budde et al., 2016). Again, bulk chondrites have fairly constant  $\epsilon^{183}\text{W}$  compositions, excluding substantial loss of either chondrules or matrix during chondrite accretion. However, complementarity by no means excludes that material with a CI-chondritic composition has been added to a given mixture of chondrules and matrix. Such an addition would not change the bulk chemical composition of the final chondrite, because material with the same chemical composition is added (Jacquet et al., 2016). For elements that do not exhibit large-scale nucleosynthetic isotope anomalies (such as  $^{183}\text{W}$ ), the addition of CI-like material would also not change the bulk isotopic composition of the final chondrite significantly.

The observations of chemical and isotopic complementarity may be reconciled with the presence of CI-like matrix in all carbonaceous chondrites if two kinds of matrices were present, namely 'chondrule-related matrix' and CI-like matrix (Braukmüller et al., 2018; Jacquet et al., 2016). The chemical and isotopic composition of chondrule-related matrix would then be complementary to those of the chondrules. As such, chondrule-related matrix would most likely represent remaining chondrule precursor dust which has not been processed into chondrules. Although the good agreement between the inferred amount of CI-like matrix and the actually observed matrix mass fractions suggests that there cannot be much chondrule-related matrix (Alexander, 2019), the uncertainties on calculated matrix mass fraction are sufficiently large to allow for the presence of some chondrule-related matrix (on the order of 10 wt.%). Alternatively, chondrule-matrix complementarity may also reflect fractionation between chondrules and their associated rims, which subsequently chemically reacted with CI-like matrix (Van Kooten et al., 2019). In this case, no chondrule-related matrix would be needed. Finally, if the mixing between chondrule precursor and CI-like dust occurred prior to chondrule formation (see above), then chondrule-matrix complementarity would naturally be preserved because all components that were not incorporated into chondrules would afterwards be mixed with the remaining unprocessed CI-like matrix. Thus, the presence of CI-like matrix in all carbonaceous chondrites is not inconsistent with chondrule-matrix complementarity.

#### 4.4. Volatile depletion in carbonaceous chondrites

##### 4.4.1. Volatile fractionation among bulk carbonaceous chondrites

The isotopic evidence for mixing between volatile-rich matrix and volatile-depleted chondrules (or chondrule precursors) among bulk carbonaceous chondrites is reminiscent of the original two-component mixing model for the volatile element variations among chondrites (Larimer and Anders, 1967). In the simplest form of this model, volatile elements in carbonaceous chondrites derive entirely from CI-like matrix, and variable volatile contents would solely reflect dilution through the addition of volatile-free chondrules. This seems consistent with the observation that in plots of volatile concentration versus matrix volume fraction, carbonaceous chondrites define linear trends which pass

through the origin (Alexander, 2019), and also with the observation that in spite of variable volatile element depletions, elements with condensation temperatures below  $\sim 750$  K always occur in CI-chondritic relative proportions (Braukmüller et al., 2018). If volatiles would indeed solely derive from CI-like matrix, then all carbonaceous chondrites would have the same, CI-like  $\delta^{128/126}\text{Te}$ . However, this present study reveals that carbonaceous chondrites have systematically variable  $\delta^{128/126}\text{Te}$  (Fig. 1), indicating more than one source for Te in carbonaceous chondrites.

Plots of volatile element concentrations (Table S4) against the mass fraction of matrix (and not volume fraction) reveal that the non-matrix component of carbonaceous chondrites, albeit depleted, is not completely devoid of volatile elements (Fig. 4). This observation holds for a large set of volatile elements (Fig. 7, Table 2) and demonstrates that volatile elements with  $T_C < 750$  K occur in CI-like relative proportions in the non-matrix component (i.e., chondrule or chondrule precursors) with an overall abundance of  $\sim 0.13 \times \text{CI}$  (Fig. 8). Thus, the different volatile element concentrations in carbonaceous chondrites reflect mixing between volatile-rich matrix and volatile-depleted chondrules/chondrule precursors, and both mixing endmembers have CI-like relative proportions of these elements. This naturally accounts for the observation that volatile elements with  $T_C < 750$  K occur in different absolute but always CI-like relative proportions in carbonaceous chondrites. As a result, and contrary to previous suggestions (Braukmüller et al., 2018), CI-like ratios of these elements in carbonaceous chondrites do not require that these elements entirely derive from CI-like matrix.

##### 4.4.2. Volatile depletion in chondrules and chondrule precursors

The correlation of  $\delta^{128/126}\text{Te}$  with Te concentration and matrix mass fraction among bulk carbonaceous chondrites suggests that chondrules in carbonaceous chondrites are isotopically light for Te. This observation is not restricted to Te, but has also been made for several other volatile elements, including Zn (Luck et al., 2005; Pringle et al., 2017), Cu (Luck et al., 2003), Ga (Kato and Moynier, 2017), and Rb (Pringle and Moynier, 2017). Collectively these data indicate that an isotopically light composition of volatile elements is a ubiquitous feature of chondrules from carbonaceous chondrites. The light isotopic composition cannot reflect volatile loss during evaporation from chondrule melts, which is expected to result in heavy isotopic compositions. The lack of heavy isotopic compositions for volatile elements has been interpreted to reflect gas-chondrule exchange or high dust-to-gas ratios (Alexander et al., 2008), both of which may have suppressed kinetic isotope fractionation. This process, however, does not by itself account for isotopically light compositions of chondrules. Pringle et al. (2017) proposed that removal of sulfides with isotopically heavy Zn may account for the light Zn isotopic composition of chondrules. As Zn and Te probably behaved quite similarly, this process may also account for the observed Te isotope systematics. This process invokes different depletion processes for moderately volatile elements with different geochemical character, as only chalcophile elements like Zn and Te could be removed by sulfide loss. However, carbonaceous chondrites are depleted in all volatile elements irrespective of their geochemical character, making it quite unlikely that different volatile elements have been lost from chondrules (or their precursors) by distinct processes. Instead, the constant depletion and CI-like ratios for all elements with  $T_C < 750$  K requires a process that affected all these elements in a similar manner.

Condensation is expected to result in light isotopic compositions because light isotopes enter the condensates at a greater rate than heavy isotopes (Richter, 2004). For instance, Marrocchi et al. (2019) observed light Si isotopic compositions for AOAs, which these authors attributed to rapid condensation of the AOAs. The light Te isotopic composition inferred for chondrules/chon-

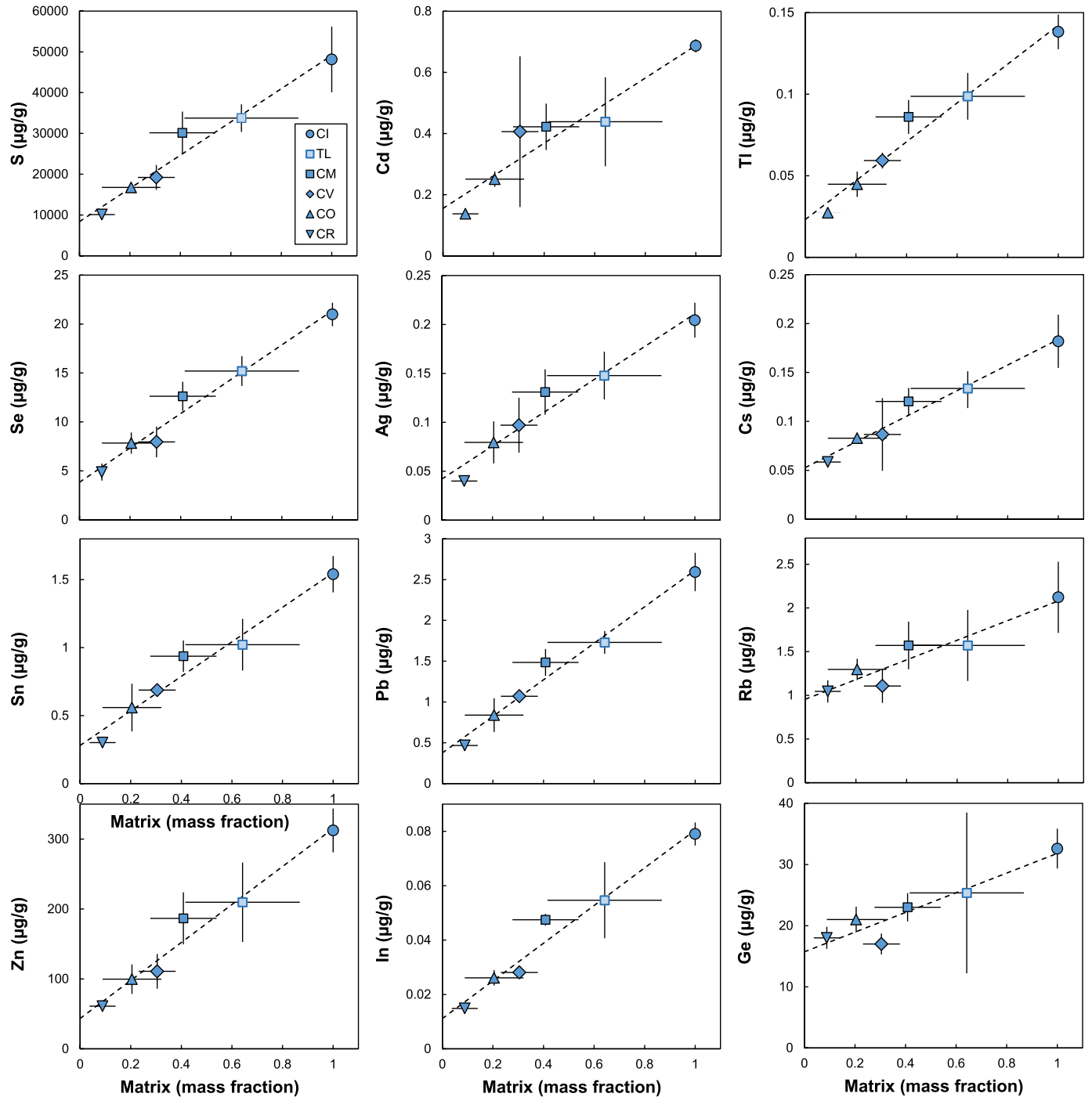


**Fig. 7.** Average concentrations of volatile elements of carbonaceous chondrite groups (Table S4) versus mass fraction of matrix (see section 4.1). Regressions represent best fits using weighted errors. For all elements, concentrations are well correlated with the amount of matrix, resulting in precise y-axis intercepts and concentrations for the non-matrix component (Table 2).

drule precursors in the present study may have a similar origin and could either reflect the partial re-condensation of volatile elements into chondrule melts or the rapid condensation of (some) chondrule precursors. However, the CI-like ratios for volatile elements with  $T_C < 750$  K in chondrules/chondrule precursors require bulk condensation from a gas with CI-like relative proportions for these elements, and so the preservation of an isotopic signature related to condensation is somewhat unexpected. Reconciling these observations, therefore, requires a two-stage process, in which rapid condensation first induced a large kinetic isotopic fractionation, which was subsequently diluted by the ad-

dition of material with CI-like ratios for volatile elements. This initial isotopic fractionation may have occurred during partial re-condensation of volatile elements into chondrule melts, but to also account for the CI-like ratios for elements with  $T_C < 750$  K, it would additionally be required that most of these elements re-condensed together before the gas became chemically fractionated. This specific pathway of evaporation and re-condensation during chondrule melting seems somewhat unlikely, and so a perhaps more straightforward interpretation may be that the light isotopic composition of chondrules is unrelated to chondrule formation itself, but is a signature of chondrule precursors, which consisted of

**Table 2**

Volatile element abundances in the non-matrix (i.e., chondrule) component of carbonaceous chondrites. All data are in  $\mu\text{g/g}$  and uncertainties are two standard deviations.

S	6524 $\pm$ 2400
Se	3.47 $\pm$ 1.10
Te	0.354 $\pm$ 0.100
Zn	36.8 $\pm$ 15.0
Cd	0.0950 $\pm$ 0.0310
Sn	0.209 $\pm$ 0.069
Pb	0.296 $\pm$ 0.120
Ag	0.0272 $\pm$ 0.0096
In	0.0088 $\pm$ 0.0034
Tl	0.0185 $\pm$ 0.0060
Cs	0.0474 $\pm$ 0.0079
Bi	0.0255 $\pm$ 0.0180
Rb	0.940 $\pm$ 0.140
Ga	4.90 $\pm$ 1.70
Ge	15.1 $\pm$ 4.6

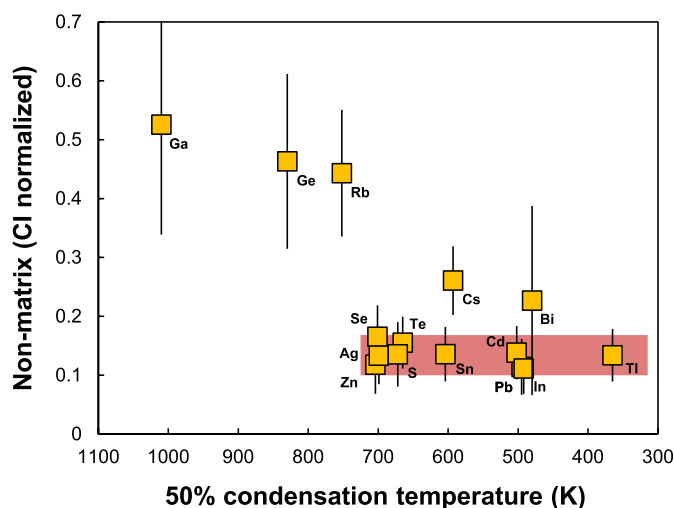


**Fig. 8.** CI-normalized volatile element abundances in the non-matrix (i.e., chondrule or chondrule precursor) component inferred from the correlations in Fig. 7 as a function of their 50% condensation temperature  $T_C$  (Wood et al., 2019). Volatile elements with  $T_C < 750$  K are present in CI chondritic relative abundances. The red bar represents the average volatile depletion of  $0.13 \pm 0.03 \times \text{CI}$  (2s.d) for these elements in the non-matrix component of carbonaceous chondrites.

isotopically light condensates mixed with isotopically unfractionated dust.

#### 4.4.3. Comparison to volatile element depletion of bulk silicate Earth

The depletion of volatile elements with  $T_C < 750$  K in chondrules/chondrule precursors is remarkably similar to the inferred depletion of these elements in the bulk silicate Earth (BSE) of  $0.10\text{--}0.15 \times \text{CI}$  (Braukmüller et al., 2019). Many of these elements are siderophile or chalcophile and are, therefore, fractionated in the BSE as a result of core formation. Nevertheless, the ratio of lithophile volatile elements like Zn and In are CI-like, suggesting that volatile elements with  $T_C < 750$  K originally occurred in CI-like ratios, and were subsequently fractionated by core formation (Braukmüller et al., 2019). On this basis, Braukmüller et al. (2019) suggested that the abundances of elements with  $T_C < 750$  K in the Earth reflect the addition of 10–15 wt.% CI-like material before cessation of core formation. The results of this study reveal, however, that the CI-like ratios of volatile elements ( $T_C < 750$  K) do not allow identifying a specific type of carbonaceous chondrites as the source of these elements. This is because volatile-poor chondrules/chondrule precursors exhibit the same CI-like ratios for these elements than CI chondrites themselves. This does not

mean that Earth accreted from volatile-poor, chondrule-like material (Hewins and Herzberg, 1996), but merely reveals that the CI-like ratios of volatile elements in the BSE may result from the accretion of volatile-depleted materials and do not require accretion of CI chondrites themselves.

## 5. Conclusions

The carbonaceous chondrite groups CI, CM, CV, CO, and CR together with the ungrouped chondrite Tagish Lake display systematic mass-dependent Te isotope variations that correlate with Te concentrations and the mass fractions of matrix in each chondrite. These trends indicate that volatile element depletion in carbonaceous chondrites is associated with mass-dependent isotope fractionation towards lighter isotopic compositions. The Te isotopic compositions are also correlated with nucleosynthetic  $\epsilon^{54}\text{Cr}$  anomalies, and bulk CV, CO, and CM chondrites as well as Tagish Lake plot on a mixing line between chondrules/chondrule precursors and CI chondrites. Together these data indicate that the variable chemical and isotopic compositions of bulk carbonaceous chondrites can be attributed to mixing between CI-like matrix and chondrules or chondrule precursors. The former is volatile-rich, isotopically heavy, and  $^{54}\text{Cr}$ -enriched, whereas the latter component is volatile-depleted, isotopically light, and has smaller  $\epsilon^{54}\text{Cr}$  anomalies.

The  $\delta^{128/126}\text{Te}\text{--}\epsilon^{54}\text{Cr}$  correlation implies that chondrules did not form from CI-like dust, but from precursors with smaller  $\epsilon^{54}\text{Cr}$  anomalies. Moreover, chondrules from the CM, CV, and CO chondrites as well as Tagish Lake derive from the same or a similar population of precursor dust. By contrast, CR chondrites deviate from the  $\delta^{128/126}\text{Te}\text{--}\epsilon^{54}\text{Cr}$  correlation defined by the other carbonaceous chondrites, indicating that the precursors of CR chondrules are isotopically distinct from those of CO, CV, and CM chondrules. As such, CR chondrites probably derive from a distinct area of the disk and/or formed later than most other carbonaceous chondrites.

Linear regressions of volatile element concentrations with the mass fraction of matrix reveal that chondrules are volatile element-depleted ( $\sim 0.13 \times \text{CI}$ ), but nevertheless contain elements with condensation temperatures below  $\sim 750$  K in approximately CI-chondritic ratios. Variable mixing of chondrules and CI-like matrix therefore naturally results in CI-like ratios for these elements in all carbonaceous chondrites, irrespective of the degree of volatile depletion. Thus, CI-like ratios of these elements do not imply that volatile elements in carbonaceous chondrites solely derive from CI-like matrix. A corollary of this observation is that the CI-like ratios of volatile elements in the bulk silicate Earth do not require accretion of volatile-rich CI-like objects to a volatile-free proto-Earth but could also reflect the accretion of variably volatile-depleted materials.

## CRedit authorship contribution statement

**Jan L. Hellmann:** Conceptualization, Investigation, Methodology, Validation, Visualization, Writing - original draft. **Timo Hopp:** Methodology, Validation, Writing - review & editing. **Christoph Burkhardt:** Conceptualization, Funding acquisition, Supervision, Writing - review & editing. **Thorsten Kleine:** Conceptualization, Funding acquisition, Resources, Supervision, Writing - original draft.

## Declaration of competing interest

The authors declare that they have no known competing financial interests or personal relationships that could have appeared to influence the work reported in this paper.

## Acknowledgements

Constructive reviews by two anonymous reviewers, and the efficient editorial handling by R. Dasgupta are gratefully acknowledged. Some of the meteorite samples for this study were provided by NASA, the Field Museum in Chicago, and the Institut de Physique du Globe de Paris in France, which is also gratefully acknowledged. We also thank A. Bischoff and E.H. Haiderer for providing the two CI chondrites Orgueil and Ivuna. Antarctic meteorite samples are recovered by the Antarctic Search for Meteorites (ANSMET) program which has been funded by NSF and NASA, and characterized and curated by the Department of Mineral Sciences of the Smithsonian Institution and Astromaterials Curation Office at NASA Johnson Space Center. Funded by the Deutsche Forschungsgemeinschaft (DFG, German Research Foundation) – Project-ID 263649064 – TRR 170. This is TRR170 publication No. 106.

## Appendix A. Supplementary material

Supplementary material related to this article can be found online at <https://doi.org/10.1016/j.epsl.2020.116508>.

## References

- Abreu, N.M., Bullock, E.S., 2013. Opaque assemblages in CR2 Graves Nunataks (GRA) 06100 as indicators of shock-driven hydrothermal alteration in the CR chondrite parent body. *Meteorit. Planet. Sci.* 48, 2406–2429.
- Albarede, F., 2009. Volatile accretion history of the terrestrial planets and dynamic implications. *Nature* 461, 1227–1233.
- Alexander, C.M.O.D., 2005. Re-examining the role of chondrules in producing the elemental fractionations in chondrites. *Meteorit. Planet. Sci.* 40, 943–965.
- Alexander, C.M.O.D., 2019. Quantitative models for the elemental and isotopic fractionations in chondrites: the carbonaceous chondrites. *Geochim. Cosmochim. Acta* 254, 277–309.
- Alexander, C.M.O.D., Boss, A., Carlson, R., 2001. The early evolution of the inner solar system: a meteoritic perspective. *Science* 293, 64–68.
- Alexander, C.M.O.D., Grossman, J.N., Ebel, D., Ciesla, F., 2008. The formation conditions of chondrules and chondrites. *Science* 320, 1617–1619.
- Anders, E., 1964. Origin, age, and composition of meteorites. *Space Sci. Rev.* 3, 583–714.
- Blinova, A.I., Zega, T.J., Herd, C.D., Stroud, R.M., 2014. Testing variations within the Tagish Lake meteorite—I: mineralogy and petrology of pristine samples. *Meteorit. Planet. Sci.* 49, 473–502.
- Bonal, L., Quirico, E., Bourot-Denise, M., Montagnac, G., 2006. Determination of the petrologic type of CV3 chondrites by Raman spectroscopy of included organic matter. *Geochim. Cosmochim. Acta* 70, 1849–1863.
- Braukmüller, N., Wombacher, F., Funk, C., Münker, C., 2019. Earth's volatile element depletion pattern inherited from a carbonaceous chondrite-like source. *Nat. Geosci.* 12, 564–568.
- Braukmüller, N., Wombacher, F., Hezel, D.C., Escoube, R., Münker, C., 2018. The chemical composition of carbonaceous chondrites: implications for volatile element depletion, complementarity and alteration. *Geochim. Cosmochim. Acta* 239, 17–48.
- Brennecka, G.A., Borg, L.E., Romaniello, S.J., Souders, A.K., Shollenberger, Q.R., Marks, N.E., Wadhwa, M., 2017. A renewed search for short-lived  $^{126}\text{Sn}$  in the early Solar System: hydride generation MC-ICPMS for high sensitivity Te isotopic analysis. *Geochim. Cosmochim. Acta* 201, 331–344.
- Briani, G., Quirico, E., Gounelle, M., Paulhiac-Pison, M., Montagnac, G., Beck, P., Orthous-Daunay, F.-R., Bonal, L., Jacquet, E., Kearsley, A., 2013. Short duration thermal metamorphism in CR chondrites. *Geochim. Cosmochim. Acta* 122, 267–279.
- Budde, G., Kleine, T., Kruijer, T.S., Burkhardt, C., Metzler, K., 2016. Tungsten isotopic constraints on the age and origin of chondrules. *Proc. Natl. Acad. Sci. USA* 113, 2886–2891.
- Budde, G., Kruijer, T.S., Kleine, T., 2018. Hf-W chronology of CR chondrites: implications for the timescales of chondrule formation and the distribution of  $^{26}\text{Al}$  in the solar nebula. *Geochim. Cosmochim. Acta* 222, 284–304.
- Ciesla, F.J., 2008. Radial transport in the solar nebula: implications for moderately volatile element depletions in chondritic meteorites. *Meteorit. Planet. Sci.* 43, 639–655.
- Desch, S., Ciesla, F., Hood, L., Nakamoto, T., 2005. Heating of chondritic materials in solar nebula shocks. In: *Chondrites and the Protoplanetary Disk*, pp. 849–872.
- Engineering ToolBox, 2001. <https://www.engineeringtoolbox.com>. (Accessed 14 February 2020).
- Fehr, M.A., Hammond, S.J., Parkinson, I.J., 2018. Tellurium stable isotope fractionation in chondritic meteorites and some terrestrial samples. *Geochim. Cosmochim. Acta* 222, 17–33.
- Fehr, M.A., Rehkämper, M., Halliday, A.N., 2004. Application of MC-ICPMS to the precise determination of tellurium isotope compositions in chondrites, iron meteorites and sulfides. *Int. J. Mass Spectrom.* 232, 83–94.
- Fehr, M.A., Rehkämper, M., Halliday, A.N., Schönbächler, M., Hattendorf, B., Günther, D., 2006. Search for nucleosynthetic and radiogenic tellurium isotope anomalies in carbonaceous chondrites. *Geochim. Cosmochim. Acta* 70, 3436–3448.
- Fukami, Y., Kimura, J.-I., Suzuki, K., 2018. Precise isotope analysis of tellurium by inductively coupled plasma mass spectrometry using a double spike method. *J. Anal. At. Spectrom.* 33, 1233–1242.
- Geiger, T., Bischoff, A., 1991. The CK chondrites—conditions of parent body metamorphism. *Meteoritics* 26, 337.
- Hewins, R.H., Herzberg, C.T., 1996. Nebular turbulence, chondrule formation, and the composition of the Earth. *Earth Planet. Sci. Lett.* 144, 1–7.
- Hezel, D.C., Palme, H., 2010. The chemical relationship between chondrules and matrix and the chondrule matrix complementarity. *Earth Planet. Sci. Lett.* 294, 85–93.
- Hildebrand, A.R., McCausland, P.J., Brown, P.G., Longstaffe, F.J., Russell, S.D., Tagliaferri, E., Wacker, J.F., Mazur, M.J., 2006. The fall and recovery of the Tagish Lake meteorite. *Meteorit. Planet. Sci.* 41, 407–431.
- Hopp, T., Kleine, T., 2018. Nature of late accretion to Earth inferred from mass-dependent Ru isotopic compositions of chondrites and mantle peridotites. *Earth Planet. Sci. Lett.* 494, 50–59.
- Jacquet, E., Barrat, J.A., Beck, P., Caste, F., Gattacceca, J., Sonzogni, C., Gounelle, M., 2016. Northwest Africa 5958: a weakly altered CM-related ungrouped chondrite, not a CI 3. *Meteorit. Planet. Sci.* 51, 851–869.
- Jacquet, E., Pignatale, F.C., Chaussidon, M., Charnoz, S., 2019. Fingerprints of the protosolar cloud collapse in the Solar System. II. Nucleosynthetic anomalies in meteorites. *Astrophys. J.* 884, 32–42.
- Kato, C., Moynier, F., 2017. Gallium isotopic evidence for the fate of moderately volatile elements in planetary bodies and refractory inclusions. *Earth Planet. Sci. Lett.* 479, 330–339.
- Larimer, J.W., Anders, E., 1967. Chemical fractionations in meteorites—II. Abundance patterns and their interpretation. *Geochim. Cosmochim. Acta* 31, 1239–1270.
- Luck, J.-M., Othman, D.B., Albarède, F., 2005. Zn and Cu isotopic variations in chondrites and iron meteorites: early solar nebula reservoirs and parent-body processes. *Geochim. Cosmochim. Acta* 69, 5351–5363.
- Luck, J.-M., Othman, D.B., Barrat, J., Albarède, F., 2003. Coupled  $^{63}\text{Cu}$  and  $^{16}\text{O}$  excesses in chondrites. *Geochim. Cosmochim. Acta* 67, 143–151.
- Macke, R.J., Consolmagno, G.J., Britt, D.T., 2011. Density, porosity, and magnetic susceptibility of carbonaceous chondrites. *Meteorit. Planet. Sci.* 46, 1842–1862.
- Mahan, B., Moynier, F., Beck, P., Pringle, E.A., Siebert, J., 2018. A history of violence: insights into post-accretionary heating in carbonaceous chondrites from volatile element abundances, Zn isotopes and water contents. *Geochim. Cosmochim. Acta* 220, 19–35.
- Marrocchi, Y., Gounelle, M., Blanchard, I., Caste, F., Kearsley, A.T., 2014. The Paris CM chondrite: secondary minerals and asteroidal processing. *Meteorit. Planet. Sci.* 49, 1232–1249.
- Marrocchi, Y., Villeneuve, J., Jacquet, E., Piralla, M., Chaussidon, M., 2019. Rapid condensation of the first Solar System solids. *Proc. Natl. Acad. Sci. USA* 116, 23461–23466.
- McSween, H.Y., 1977a. Carbonaceous chondrites of the Ornans type: a metamorphic sequence. *Geochim. Cosmochim. Acta* 41, 477–491.
- McSween, H.Y., 1977b. Petrographic variations among carbonaceous chondrites of the Vigarano type. *Geochim. Cosmochim. Acta* 41, 1777–1790.
- McSween, H.Y., 1979. Alteration in CM carbonaceous chondrites inferred from modal and chemical variations in matrix. *Geochim. Cosmochim. Acta* 43, 1761–1770.
- Olsen, M.B., Wielandt, D., Schiller, M., Van Kooten, E.M., Bizzarro, M., 2016. Magnesium and  $^{54}\text{Cr}$  isotope compositions of carbonaceous chondrite chondrules—Insights into early disk processes. *Geochim. Cosmochim. Acta* 191, 118–138.
- Palme, H., Lodders, K., Jones, A., 2014. Solar System abundances of the elements. In: Davis, A.M. (Ed.), *Treatise on Geochemistry*, 2 ed. Elsevier, Oxford, pp. 41–61.
- Pringle, E.A., Moynier, F., 2017. Rubidium isotopic composition of the Earth, meteorites, and the Moon: evidence for the origin of volatile loss during planetary accretion. *Earth Planet. Sci. Lett.* 473, 62–70.
- Pringle, E.A., Moynier, F., Beck, P., Paniello, R., Hezel, D.C., 2017. The origin of volatile element depletion in early solar system material: clues from Zn isotopes in chondrules. *Earth Planet. Sci. Lett.* 468, 62–71.
- Richter, F.M., 2004. Timescales determining the degree of kinetic isotope fractionation by evaporation and condensation. *Geochim. Cosmochim. Acta* 68, 4971–4992.
- Rudge, J.F., Reynolds, B.C., Bourdon, B., 2009. The double spike toolbox. *Chem. Geol.* 265, 420–431.
- Schrader, D.L., Franchi, I.A., Connolly Jr., H.C., Greenwood, R.C., Lauretta, D.S., Gibson, J.M., 2011. The formation and alteration of the Renazzo-like carbonaceous chondrites I: implications of bulk-oxygen isotopic composition. *Geochim. Cosmochim. Acta* 75, 308–325.

- Siebert, C., Nögler, T.F., Kramers, J.D., 2001. Determination of molybdenum isotope fractionation by double-spike multicollector inductively coupled plasma mass spectrometry. *Geochem. Geophys. Geosyst.* 2, 2000GC000124.
- Toth, E.R., Fehr, M.A., Friebel, M., Schönbächler, M., 2020. Cadmium isotopes in chondrites and acid leachates: nucleosynthetic homogeneity and a monitor for thermal neutron capture effects. *Geochim. Cosmochim. Acta* 274, 286–301.
- Trinquier, A., Birck, J.-L., Allegre, C.J., 2007. Widespread  $^{54}\text{Cr}$  heterogeneity in the inner solar system. *Astrophys. J.* 655, 1179–1185.
- Trinquier, A., Elliott, T., Ulfbeck, D., Coath, C., Krot, A.N., Bizzarro, M., 2009. Origin of nucleosynthetic isotope heterogeneity in the solar protoplanetary disk. *Science* 324, 374–376.
- Van Kooten, E., Cavalcante, L., Wielandt, D., Bizzarro, M., 2020. The role of Bells in the continuous accretion between the CM and CR chondrite reservoirs. *Meteorit. Planet. Sci.*, 1–16.
- Van Kooten, E.M., Moynier, F., Agranier, A., 2019. A unifying model for the accretion of chondrules and matrix. *Proc. Natl. Acad. Sci. USA* 116, 18860–18866.
- Van Kooten, E.M.M.E., Moynier, F., 2019. Zinc isotope analyses of singularly small samples (<5 ng Zn): investigating chondrule-matrix complementarity in Leoville. *Geochim. Cosmochim. Acta* 261, 248–268.
- Wasson, J.T., Chou, C.L., 1974. Fractionation of moderately volatile elements in ordinary chondrites. *Meteoritics* 9, 69–84.
- Wombacher, F., Rehkämper, M., Mezger, K., Bischoff, A., Münker, C., 2008. Cadmium stable isotope cosmochemistry. *Geochim. Cosmochim. Acta* 72, 646–667.
- Wood, B.J., Smythe, D.J., Harrison, T., 2019. The condensation temperatures of the elements: a reappraisal. *Am. Mineral. J. Earth Planet. Mater.* 104, 844–856.
- Zanda, B., Lewin, É., Humayun, M., 2018. The chondritic assemblage: complementarity is not a required hypothesis. In: Russell, S.S., Connolly Jr., H.C., Krot, A.N. (Eds.), *Chondrules - Records of Protoplanetary Disk Processes*. Cambridge University Press, Cambridge, pp. 122–150.